ISSN: 0976-3031

Available Online at http://www.recentscientific.com

International Journal of Recent Scientific Research
Vol. 7, Issue, 9, pp. 13462-13473, September, 2016

International Journal of Recent Scientific Research

Research Article

STUDY OF THE STRUCTURAL MODIFICATIONS OF CYCLOPHOSPHATES OF MANGANESE FROM $M_3(P_3O_9)_2.10H_2O$ TO $Mn_2P_4O_{12}$ DURING THERMAL BEHAVIOR PROCESS BY INFRARED SPECTROSCOPY

Bouchra Gourja[1,2]., Mustafa Belhabra[1]., Malika Tridane[1,2] and Said Belaaouad[1]

[1]Laboratoire de Chimie Physique des Matériaux, Faculté des Sciences Ben M'sik, Université Hassan II de Casablanca, Casablanca, Maroc
[2]Centre Régional des métiers d'enseignement et de formation Casablanca Anfa, Bd Bir Anzarane Casablanca. Maroc

ARTICLE INFO

Article History:
Received 05th June, 2016
Received in revised form 21st July, 2016
Accepted 06th August, 2016
Published online 28th September, 2016

Key Words:
Chemical preparation, thermal behavior, structural modifications, infrared spectrometry, chemical analyses, kinetic study, thermal analyses (TGA-DTA), differential scanning calorimetry (DSC), X-ray diffraction.

ABSTRACT

Chemical preparation, thermal behavior, kinetic and IR studies are given for the cyclotriphosphate $Mn_3(P_3O_9)_2.10H_2O$. $Mn_3(P_3O_9)_2.10H_2O$, which has already been studied, is monoclinic $P2_1/n$ with the following unit-cell dimensions : a = 9.631(5)Å,b = 18,173(7)Å, c = 7,976(4), β = 109,438(4)° and Z = 2. The study of the structural modifications of cyclophosphates of manganese from $Mn_3(P_3O_9)_2.10H_2O$ to $Mn_2P_4O_{12}$ during thermal behavior process by infrared spectroscopy has never been performed. It's the first time where a cyclotriphosphate P_3O_9 is converted to a cyclotetraphosphate P_4O_{12} by thermal dehydration. The thermal behavior of $Mn_3(P_3O_9)_2.10H_2O$ has been investigated and interpreted by comparison with IR absorption spectrometry, X-ray diffraction experiments, chemical analyses, thermal analyses (TGA-DTA) and differential scanning calorimetry (DSC). $Mn_3(P_3O_9)_2.10H_2O$ is stable, in the conditions of temperature and pressure of our laboratory, until 70°C. It is impossible to dehydrate $Mn_3(P_3O_9)_2.10H_2O$ without breaking its rings $P_3O_9^{3-}$ and leading to amorphous compounds in X-ray diffraction and IR absorption spectrometry. The final product of the dehydration and calcination of $Mn_3(P_3O_9)_2.10H_2O$ cyclotriphosphate, under atmospheric pressure, is its cyclotetraphosphate $Mn_2P_4O_{12}$. $Mn_2P_4O_{12}$ is prepared otherwise by dry way.

INTRODUCTION

Alkaline earth cyclotriphosphates $M^{II}_3(P_3O_9)_2.nH_2O$ (M^{II} = Ca, n = 10; M^{II} = Ba, n = 6 and 4; M^{II} = Sr, n = 7 and 5; M^{II} = Cd, n = 14 and 10; M^{II} = Pb, n = 3 and M^{II} = Mn, n = 10) whose crystalline structures are known [1,2,3,4], have been studied by thermal behaviors, kinetic and IR studies [5,6,7,8]. The dehydration of these cyclotriphosphates lead generally to long-chain polyphosphates [9,10], $M^{II}(PO_3)_2$ (M^{II} = Ca, Ba, Sr, Cd and Pb), which can be used in industry such as corrosion inhibitors [11] and humidity sensor [12]. Manganese phosphates considerably possess industrial interesting properties nowadays because of their wide applications in laser host [13], ceramic [14], dielectric [15], electric [16], magnetic [17] and catalytic [18] processes. Manganese phosphates are transformed to other phosphates by hydrolysis and dehydration reactions at elevated temperatures [19-22]. $Mn_3(P_3O_9)_2.10H_2O$, $Mn(NH_4)_4(P_3O_9)_2.6H_2O$ and $Mn_2P_4O_{12}$ have wide range of applications and can be used as catalysts, ion exchangers, reactants in ionic conditions, intercalation reactions superphosphate fertilizers and as inorganic pigment in ceramics [23-31]. The cyclotriphosphate decahydrate of manganese, $Mn_3(P_3O_9)_2.10H_2O$, presented in this paper is stable under the conditions of temperature and pressure of our laboratory. The present work deals with a synthesis, thermal behavior, kinetic and IR studies of the cyclotriphosphate $Mn_3(P_3O_9)_2.10H_2O$.

Experimental

Chemical Preparation

Polycrystalline samples of the title compound, $Mn_3(P_3O_9)_2.10H_2O$, were prepared by adding slowly dilute cyclotriphosphoric acid to an aqueous solution of manganese carbonate, according to the following chemical reaction :

$$2H_3P_3O_9 + 3MnCO_3 + 7H_2O \longrightarrow Mn_3(P_3O_9)_2.10H_2O + 3CO_2$$

The so-obtained solution was then slowly evaporated at room temperature until polycrystalline samples of $Mn_3(P_3O_9)_2.10H_2O$

*Corresponding author: **Bouchra Gourja***
Laboratoire de Chimie Physique des Matériaux, Faculté des Sciences Ben M'sik, Université Hassan II de Casablanca, Casablanca, Maroc

were obtained. The cyclotriphosphoric acid used in this reaction was prepared from an aqueous solution of $Na_3P_3O_9$ passed through an ion-exchange resin "Amberlite IR 120" [32].

Investigation

X-ray diffraction

Powder diffraction patterns were registered with a Siemens diffractometer type D 5000 using $CuK_{\alpha 1}$ radiation (λ = 1.5406Å).

Chemical analyses

Chemical analyses were performed on a spectrophotometer of atomic absorption type VARIAN AA-475.

Infrared spectroscopy

Spectra were recorded in the range 4000-400 cm^{-1} with a Perkin-Elmer IR 983G spectrophotometer, using samples dispersed in spectroscopically pure KBr pellets and in the range 600 – 30 cm^{-1} with Bruker IF S66V/S spectrophotometer.

Thermal behaviour

Thermal analyses TGA-DTA coupled were performed using the multimodule 92 Setaram Analyzer operating from room temperature up to 1400°C, in a platinum crucible, at various heating rates from 1 to 15°C/min.

Differential scanning calorimetry (DSC) was carried out with a Setaram DSC 92 apparatus.

RESULTS AND DISCUSSION

Crystal data, chemical analyses and dehydration

$Mn_3(P_3O_9)_2.10H_2O$ is monoclinic $P2_1/n$ with the following unit-cell dimensions:

a = 9.631(5)Å, b = 18,173(7)Å, c = 7,976 (4), β = 109,438(4)° and Z = 2 [1]. $Mn_3(P_3O_9)_2.10H_2O$ has never been studied except its crystallographic characterization.

The results of the chemical analyses and dehydration of the title compound are in total accordance with the formula $Mn_3(P_3O_9)_2.10H_2O$ and are gathered in Table 1.

Table 1 Results of the chemical analyses and dehydration of $Mn_3(P_3O_9)_2.10H_2O$

P / Mn		H_2O	
theoretical	experimental	theoretical	experimental
2	2.002	10	10.003

Stability

The cyclotriphosphate decahydrate of manganese, $Mn_3(P_3O_9)_2.10H_2O$, is stable in the conditions of temperature and pressure of our laboratory until 80°C. We have followed, by IR spectrometry, X-ray diffraction and thermogravimetric analyses, the stability of $Mn_3(P_3O_9)_2.10H_2O$ during one year, and no evolution was observed. The X-ray diffraction pattern of $Mn_3(P_3O_9)_2.10H_2O$ is reported in Figure 1.

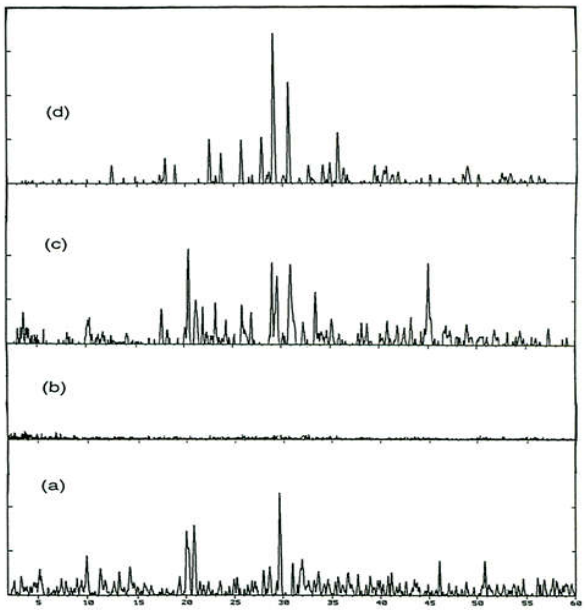

Figure 1 X-ray powder diffractograms of the phosphates (a) $Mn_3(P_3O_9)_2.10H_2O$, (b) amorphous phase, (c) mixture of $Mn_2P_4O_{12}$ and $Mn_2P_2O_7$ and (d) $Mn_2P_4O_{12}$

IR Studies

Characterization of $Mn_3(P_3O_9)_2.10H_2O$ by IR vibration spectrometry

The IR absorption spectrum of $Mn_3(P_3O_9)_2.10H_2O$ is reported in Figure 2. In the domain 4000-1600 cm^{-1}, the spectrum (a) (Figure 2a) shows five bands at 3558, 3444, 3275, 1658 and 1635 cm^{-1}. The bands at 3558, 3444 and 3275 cm^{-1} are attributed to the stretching vibrations of water molecules (νO-H). The bands at 1658 and 1635 cm^{-1} represent the bending vibration of water molecules (δHOH).

Between 1400 and 640 cm^{-1} the spectrum (a) (Figure 2a) shows valency vibration bands characteristic of phosphates with ring anions $P_3O_9^{3-}$ [33, 34, 35, 36]. Among these bands can be distinguished:

- the vibration bands of the (OPO) end groups at high frequencies : $1180 < \nu_{as}$ OPO < 1340 cm^{-1} and $1060 < \nu_s$ OPO < 1180 cm^{-1} ;
- the valency vibrations of the (P-O-P) ring groups at : $960 < \nu_{as}$ POP < 1060 cm^{-1} and $660 < \nu_s$ POP < 960 cm^{-1} ;

The valency vibrations of the (POP) ring groups are represented in the spectrum (a) (Figure 2a) by a very strong band at about 977 cm^{-1} which can be attributed to the ν_{as} POP antisymmetric vibrations and by two strong bands between 700 and 800 cm^{-1} (at 760 and 743 cm^{-1}) which can be related to the ν_s POP symmetric vibrations. These two strong bands characterize with no ambiguity the structure of a cyclotriphosphate $P_3O_9^{3-}$ [33].

Between 660 and 400 cm^{-1} the spectrum (a) (Figure 2a) shows bending vibration bands characteristic of phosphates with ring anions [33, 34, 35, 36]. The nature of the vibration

corresponding to the different observed bands is given in Table 2.

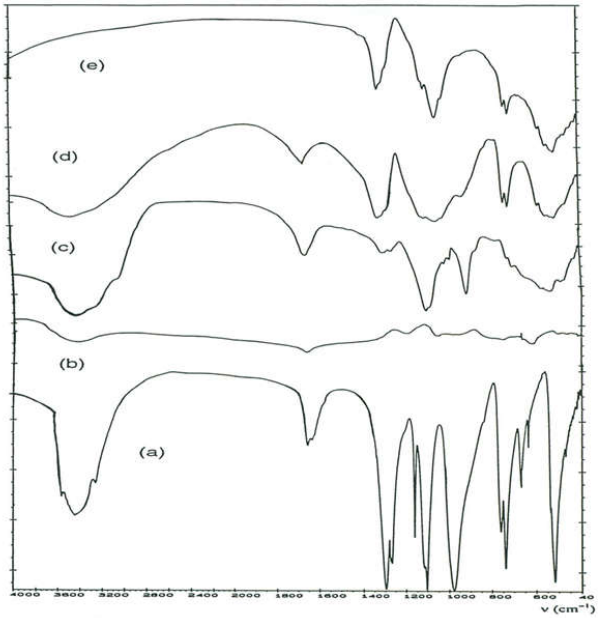

Figure 2 IR spectra of the phosphates (a) $Mn_3(P_3O_9)_2.10H_2O$, (b) amorphous phase, (c) mixture of $Mn_2P_4O_{12}$ and $Mn_2P_2O_7$ and (d) evolution to $Mn_2P_4O_{12}$ (c) $Mn_2P_4O_{12}$

Vibrational study of $Mn_3(P_3O_9)_2.10H_2O$

Interpretation of the infrared (IR) spectrum of $Mn_3(P_3O_9)_2.10H_2O$ and vibrations analysis of the four cycles $P_3O_9^{3-}$ contained in the cyclotriphosphate decahydrate of manganese, $Mn_3(P_3O_9)_2.10H_2O$.

Interpretation of the IR spectrum of the cyclotriphosphate decahydrate of manganese $Mn_3(P_3O_9)_2.10H_2O$

Analysis of the isolated P_3O_9 cycle vibrations with local symmetry C_1 [33]

The P_3O_9 cycle in the crystal of the cyclotriphosphate decahydrate of manganese $Mn_3(P_3O_9)_2.10H_2O$ [37] possesses the local symmetry C_1. The reduced representation of the internal modes of the isolated P_3O_9 ring with local symmetry C_1 [33, 34, 35] is Γcycle (C_1) = 30A, which leads to 30 normal active modes at the same time in IR and Raman (**Table 3**).

Table 2 Frequencies (cm^{-1}) of IR absorption bands for $Mn_3(P_3O_9)_2.10H_2O$

ν(cm^{-1})	Vibration
3558 3444	ν OH
1658 1635	δ HOH
1297 1274	ν_{as} OPO
1269 1166 1117 1103	ν_s OPO
977 840	ν_{as} POP
760 743	ν_s POP
670 537 520	δ OPO + ρ OPO

Table 3 separation of the vibration normal modes, active in IR and Raman of the isolated P_3O_9 cycle with local symmetry C_1 [12, 36]

	IR	Raman
internal vibration modes of the cycle with symmetry C_1	30A	30A
stretching modes	12A	12A
bending modes	18A	18A

Analysis of the vibrations of the 4 cycles in interaction

The unit-cell of the cyclotriphosphate Mn_3 $(P_3O_9)_2.10H_2O$ contains four P_3O_9 cycles. Indeed, this cyclotriphosphate crystallizes in the monoclinic system, space group $P2_1/n$ (C^5_{2h}), Z=2 [1, 37].

Theoretical group analysis leads to the results of the **Table 4** by using the following simplified hypotheses of work:

- the water molecule is supposed to be a specific ion and the internal modes of vibrations of H_2O are separated from the other normal modes of vibration,
- during modes of low frequency, the cycles move without bending. This means that there is a possibility of separating the network vibration modes (Γ network) from the internal vibration modes of the four cycles contained in the unit-cell,
- finally, within the internal vibration modes of the four cycles (Γ vibration) one can separate the stretching vibrations from bending vibrations of the cycles.

Table 4 Separation of the normal modes of vibration, IR activities and Raman of the cycles P_3O_9 in $Mn_3(P_3O_9)_2.10H_2O$.

	IR	Raman
internal vibration modes of the cycle	$30A_u + 30B_u$	$30A_g + 30B_g$
stretching modes	$12A_u + 12B_u$	$12A_g + 12B_g$
bending modes	$18A_u + 18B_u$	$18A_g + 18B_g$

When the analysis is carried out on the basis of group factor C_{2h}, by taking account the possible vibrational couplings between the four cycles of the unit-cell, it leads to the existence of 60 modes active in IR (30Au + 30 Bu) and this much in Raman (30Ag + 30 Bg) (**Table 4**). In consequence of the existence of a center of symmetry of the group factor C_{2h}, no active mode in IR isn't in Raman and vice versa. During the passage from the isolated cycle with C_1 symmetry to the crystalline unit-cell, each band of mode A should lead to a doublet as well as in IR ($A_u + B_u$) than in Raman ($A_g + B_g$) in accordance with the following correlation diagram:

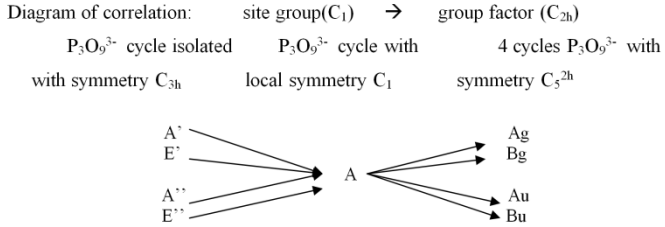

It is useful to have a precise idea about the way in which the stretching vibrational modes are corresponding for the isolated cycle P_3O_9 with symmetry C_{3h} and the isolated cycle in the crystal with site symmetry C_1 and then when the couplings are

established, possibly, between the 4 cycles in the crystal with space group $P2_1/n$ (**Table 5**). It comes out from this theoretical analysis that the possible interaction (or the vibrational couplings) between the 4 cycles $P_3O_9^{3-}$ of a unit-cell of the cyclotriphosphate decahydrate of manganese, $Mn_3(P_3O_9)_2.10H_2O$, should appear in the IR spectrum and the Raman spectrum by the existence of 6 bands in each of the four stretching vibration domains.

The IR experimental spectrum of the cyclotriphosphate decahydrate of manganese $Mn_3(P_3O_9)_2.10H_2O$ shows three frequencies in each of the 2 vibrational domains ν_{as} OPO^- and ν_s OPO^-, one shoulder in the domain ν_{as} OPO^-, one frequency in the range ν_{as} POP, three frequencies and one shoulder in the domain ν_s POP. In fact, the two vibrational domains ν_{as} OPO^- and ν_s OPO^- contain, three frequencies per range, observed respectively at (1296, 1274 and 1269 cm^{-1} and one shoulder at 1211cm^{-1}) and at (1166, 1117 and 1103 cm^{-1}). The vibrational domain of ν_{as} POP contains one frequency observed at 977 cm^{-1}. Only the vibrational range of ν_s POP contains three frequencies observed at 760, 743 and 670 cm^{-1} and one shoulder at 840 cm^{-1}.

On the basis of these results, we can say that the vibrational domains ν_{as} OPO^- (three frequencies), ν_s OPO^- (three frequencies) and ν_s POP (three frequencies) contain the same number of bands envisaged, theoretically, for an isolated cycle with site symmetry C_1 except the domain ν_{as} POP (one frequency at 977cm^{-1}) a number of bands lower than that envisaged theoretically. The theoretical analysis envisages 3 observable frequencies per field of stretching vibrations. It's the case of the three rangesν_{as} OPO^- (1297, 1274 and 1269 cm^{-1}), ν_s OPO^- (1166, 1117 and 1103 cm^{-1}) and ν_s POP (three frequencies: 760, 743 and 670 cm^{-1}). The IR spectrum of $Mn_3(P_3O_9)_2.10H_2O$ is well interpreted using local symmetry C_1 of cycle P_3O_9 presumed as isolated. The vibrational couplings do not seem to take place. The attribution of the stretching frequencies of the cycle P_3O_9 with exact local symmetry C_1 in the cyclotriphosphate $Mn_3(P_3O_9)_2.10H_2O$ is given in **Table 7**.It is to be noticed that approximate symmetry or pseudo-symmetry C_{3v} of the P_3O_9 cycle in $Mn_3(P_3O_9)_2.10H_2O$ determinated by X-ray diffraction [1, 37] and its isotypic compound $MnCa_2(P_3O_9)_2.10H_2O$ [38] , is also a good approximation making it possible to interpret the IR experimental spectrum of the cyclotriphosphate $Mn_3(P_3O_9)_2.10H_2O$. On the contrary, the IR spectrum of the cyclotriphosphate $Mn_3(P_3O_9)_2.10H_2O$ presents three frequencies in each of the three vibrations ranges ν_{as} OPO^-, ν_s OPO^- and ν_s POP, that is to say a number of frequencies higher than that planned for the approximate local symmetry C_{3v}, for which two frequencies are waited for each vibrational range, but good for the exact local symmetry C_1, for which three frequencies are waited for each vibrational domain (It's the case of the ranges ν_{as} OPO^-, ν_s OPO^- and ν_s POP which contain three frequencies in each domain.

In the IR spectra of this class of compounds analysed on the basis of the crystalline unit-cell, one must expect to observe 6 frequencies per stretching vibrations domain as well as in IR and in Raman. In all the cases, the IR observed frequencies in the IR spectra do not exceed those predicted theoretically. The IR bands characteristic of a lowering of the symmetry of the P_3O_9 cycle compared to the symmetry C_{3h} observed around 670 cm^{-1} and 1166cm^{-1} are observable in the IR spectrum of $Mn_3(P_3O_9)_2.10H_2O$ (670 and 1166 cm^{-1}). These frequencies are assigned to the simple modes A_1 of the C_{3v} symmetry or A for the site symmetry C_1. They characterize in IR a lowering of symmetry compared to the C_{3h} symmetry and are the most intense frequencies which one can expect in the Raman spectrum of all the cyclotriphosphates no matter what the symmetry of their cycle P_3O_9 is.

Table 5 Comparison of the stretching vibrational modes of the isolated cycle with local symmetry C_1 and the four cycles of the crystalline unit-cell in interaction between them in the cyclotriphosphate $Mn_3(P_3O_9)_2.10H_2O$

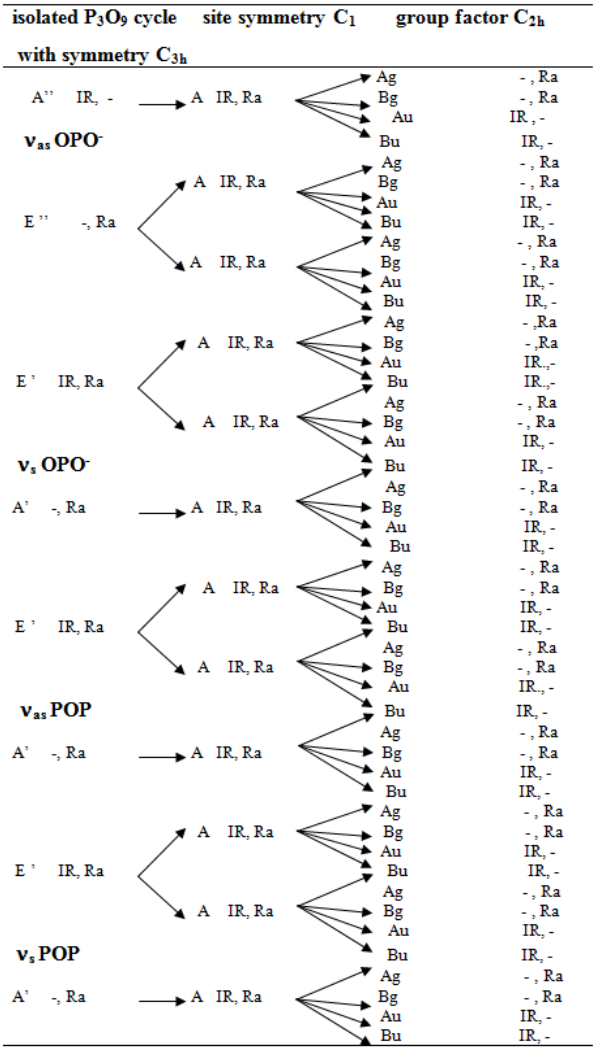

Quantum chemical calculations for the $P_3O_9^{3-}$ rings

Quantum chemical calculations have been made for the $P_3O_9^{3-}$ rings using the MNDO method (modified neglect differential overlap) [39]. The domain, 1400-650 cm^{-1}, characteristic of the valence vibration bands of the $P_3O_9^{3-}$ cycle [40], as well as possible bands due to interactions between P_3O_9 cycles and water molecules and also water vibration modes will be examined on the basis, of our results of the thirty normal IR calculated frequencies of the P_3O_9 ring with high symmetry D_{3h}, of the frequency shifts during theoretical isotopic

Table 6 Assignments of the stretching vibrations of the $P_3O_9^{3-}$ cycles with symmetry C_1 in the cyclotriphosphate $Mn_3(P_3O_9)_2.10H_2O$

Movement Mode IR Ra		IR frequencies (in cm^{-1}) observed in $Mn_3(P_3O_9)_2.10H_2O$			
C_{3v}		C_1		C_{2h}	
			3558		
			3444		
			3275		ν OH
			1658		υ_δ HOH
			1635		
IR	Ra	IR	Ra		
υ_{as} OPO					
A_1 +	+	A +	+	1297	Au Bu
		A +	+	1297	Au Bu
E +	+			1274	
		A +	+	1269	Au Bu
				1211	
υ_s OPO					
A_1 +	+	A +	+	1166	Au Bu
		A +	+		Au Bu
E +	+				
		A +	+	1117	Au Bu
				1103	
υ_{as} POP					
E +	+	A +	+	977	Au Bu
		A +	+		Au Bu
A_2 -	-	A +	+	840	Au Bu
υ_s POP					
E +	+	A +	+	760	Au Bu
		A +	+	743	Au Bu
A_1 +	+	A +	+	670	Au Bu

substitutions of the equivalent atoms (3P, 3Oi and 6Oe) belonging to the $P_3Oi_3Oe_6$ ring (D_{3h}) in relation with the proposed crystalline structure. $Mn_3(P_3O_9)_2.10H_2O$ crystallizes in the monoclinic system, space group $P2_1/n$ (C_{2h}^5), with a unit-cell containing 4 cycles P_3O_9 with local symmetry C_1. The reduced representation of the internal modes of the isolated ring P_3O_9 with D_{3h} symmetry is $\Gamma int = 4A'_1(-,Ra) + 2A'_2(-,-) + 6E'(IR,Ra) + A''_1(-,-) + 3A''_2(IR,-) + 4E''(-,Ra)$. The cycle P_3O_9 is built, theoretically, by three external (PO_2) groups and the P_3Oi_3 ring.

Theoretical group analysis leads, for the valence vibration bands (the only ones which we consider here) to $\Gamma PO_2 = A'_1(-,Ra) + A''_2(IR,-) + E'(IR,Ra) + E''(-,Ra)$ and $\Gamma P_3Oi_3 = A'_1(-,Ra) + A'_2(-,-) + 2E'(IR,Ra)$. Theoretical group analysis predicts six valence vibration bands for the PO_2 groups, six valence vibration bands for the P_3Oi_3 ring and 18 bending vibration bands for the P_3O_9 ring, $\Gamma bending = 2A'_1(-,Ra) + A'_2(-,-) + A''_1(-,-) + 2A''_2(IR,-) + 3E'(IR,Ra) + 3E''(-,Ra)$. These thirty fundamental frequencies of the cycle, D_{3h}, were calculated, by the MNDO method [39], and their attribution was made by using successive isotopic substitutions ^{16}Oi-^{18}Oi, ^{31}P-^{33}P and ^{16}Oe-^{18}Oe (**Table 7**). From the isotopic effects ($\Delta\nu$), the contribution of each group of atoms, POiP and/or PO_2, to each calculated normal frequency was determinated. With this intention, we supposed that the pure movements of the POiP groups must leave the external oxygen atoms, Oe, fixed and those due to 100% of internal groups, Oi, fixed. By means of this assumption, the percentage of participation of each group was determinated (**Table 7**).

Table 7 IR frequencies and displacements ($\Delta\nu$ in cm^{-1}) calculated for the D_{3h} symmetry and for the substitutions of the internal oxygen atoms (Oi), of the external oxygen atoms (Oe) by the isotope ^{18}O and of the phosphorus atoms by the isotope ^{33}P and percentage of participation of the POP and PO_2 groups

$^{31}P_3{}^{16}O_9{}^{3-}$	$^{31}P_3{}^{18}Oi_3{}^{16}Oe_6{}^{3-}$		$^{33}P_3{}^{16}O_9{}^{3-}$		$^{31}P_3{}^{16}Oi_3{}^{18}Oe_6{}^{3-}$		% of
ν(cm^{-1})	ν (cm^{-1})	Δν (cm^{-1})	ν (cm^{-1})	Δν (cm^{-1})	ν (cm^{-1})	Δν cm^{-1})	participation
1287.75	1287.52	0.23	1269.04	18.71	1249.67	38.08	$\upsilon_{as}PO_2$ [99]
1271.80	1271.77	0.03	1253.83	17.97	1233.02	38.78	$\upsilon_{as}PO_2$ [100]
1271.79	1271.76	0.03	1253.81	17.98	1233.01	38.78	
1225.00	1179.05	45.95	1215.39	9.61	1223.98	1.02	υ_{as}POP [98] + $\upsilon_s PO_2$ [2]
1224.94	1178.99	45.95	1215.23	9.71	1223.92	1.02	
1168.89	1168.79	0.10	1156.02	12.87	1127.56	41.33	$\upsilon_s PO_2$ [100]
1108.24	1098.42	9.82	1102.00	6.24	1062.75	45.49	υ_{as}POP [18] + $\upsilon_s PO_2$ [82]
1108.21	1098.39	9.82	1101.97	6.24	1062.72	45.49	
1059.25	1011.03	48.22	1052.97	6.28	1059.01	0.24	υ_{as} POP [100]
780.69	768.59	12.10	765.37	15.32	776.16	4.53	υ_sPOP [73] + δPO_2 [27]
780.68	768.57	12.11	765.37	15.31	776.14	4.54	
670.86	659.43	11.43	663.10	7.76	660.19	10.67	υ_sPOP [52] + δPO_2 [48]
558.95	536.78	22.17	555.05	3.90	552.77	6.18	δPOP (δcycle) [78] + δPO_2 [22]
511.25	495.99	15.26	509.05	2.20	501.27	9.98	γPOP [60] + $\gamma_R PO_2$ [40]
436.70	433.13	3.57	432.42	4.28	422.94	13.76	δPOP [21] + δPO_2 [79]
436.68	433.11	3.57	432.41	4.27	422.92	13.76	
420.07	417.52	2.55	413.15	6.92	411.17	8.90	$\gamma_W PO_2$ [78]
418.47	406.18	12.29	416.87	1.60	410.01	8.46	γPOP [59] + $\gamma_T PO_2$ [41]
418.41	406.12	12.29	416.81	1.60	409.96	8.45	
301.96	301.61	0.35	301.36	0.60	285.89	16.07	δPO_2 [98]
298.71	292.63	6.08	298.22	0.49	289.41	9.30	δPOP[40] + $\gamma_W PO_2$ [60]
298.67	292.59	6.08	298.18	0.49	289.37	9.30	
280.95	279.15	1.80	279.08	1.87	269.77	11.18	γPOP [14] + $\gamma_T PO_2$ [86]
280.92	279.11	1.81	279.05	1.87	269.74	11.18	
256.50	253.00	3.50	255.02	1.48	246.50	10.00	δPOP [26] + $\gamma_W PO_2$ [74]
256.49	252.98	3.51	255.01	1.48	246.49	10.00	
214.13	214.13	0.00	214.13	0.00	201.88	12.25	$\gamma_T PO_2$ [100]
49.08	48.30	0.78	49.08	0.00	47.01	2.07	γPOP [27] + $\gamma_R PO_2$ [73]
35.78	35.11	0.67	35.77	0.01	34.39	1.39	γPOP [33] + $\gamma_R PO_2$ [67]
34.40	33.75	0.65	34.40	0.00	33.00	1.40	

υ_{as} : asymmetric stretching; υ_s : symmetric stretching; δ : bending;
γ : out of plane P_3Oi_3; γ_W : wagging ($\gamma \perp PO_2$); γ_R : rocking (γ // PO_2); γ_T : twisting; Oi : internal oxygen atom of the ring and Oe: external oxygen atom of the ring

The geometrical parameters of the $P_3O_9^{3-}$ ring with D_{3h} symmetry, optimized by the MNDO [39] program, are comparable with those obtained, by X-ray diffraction for the compounds with known structures. The internal bond angles of the cycle, POiP, are the only parameters for which we note a variation, with more than 8.6%, relatively significant, between their values at the equilibrium obtained by MNDO [39] method and those obtained by X-ray diffraction.

This allowed us an attribution of the thirty fundamental frequencies of the cycle D_{3h} on valid theoretical bases including 12 valence vibration frequencies and 18 bending vibration frequencies. The correlation between the D_{3h} group and the site group C_1 shows that the simple normal modes, of the D_{3h} group, (A'_1, A'_2, A''_1 and A''_2) are resolved each one into the mode A of the C_1 group and the doubly degenerate E′ and E" modes are resolved into two modes A active in IR and Raman. The factor group analysis predicts for 4 cycles of the unit-cell of $Mn_3(P_3O_9)_2.10H_2O$ ($P2_1/n$, C_{2h}^5) 24 valence vibration bands active in IR. But, we observe in the IR spectrum of $Mn_3(P_3O_9)_2.10H_2O$ ($P2_1/n$, C_{2h}^5) only 7 bands and one inflection (**Figure. 2a**). It seems that the vibrational couplings between the P_3O_9 cycles of the unit-cell are absent or very weak; thus we will be able to interpret the IR spectrum, in the range 1400-650 cm^{-1}, of $Mn_3(P_3O_9)_2.10H_2O$ ($P2_1/n$, C_{2h}^5) according to the vibrations of an isolated cycle with local symmetry C_1. The values of the calculated frequencies, for the D_{3h} symmetry, are close to those observed for $Mn_3(P_3O_9)_2.10H_2O$ ($P2_1/n$, C_{2h}^5) (**Table 8**). The table 8 gives the attribution of the observed valence frequencies, 1400-650 cm^{-1}, of the P_3O_9 ring, with D_{3h} symmetry, of $Mn_3(P_3O_9)_2.10H_2O$ ($P2_1/n$, C_{2h}^5).

Thermal Behavior

Non isothermal study

The two curves corresponding to the TG and DTG analyses in air atmosphere and at a heating rate 10°C. min^{-1} of $Mn_3(P_3O_9)_2.10H_2O$ are given in **Figure 3**. The dehydration of the cyclotriphosphate hexahydrate of manganese, $Mn_3(P_3O_9)_2.10H_2O$, occurs in three steps in three temperature ranges 78 - 200°C, 200 – 322°C and 322 - 400°C (**Figure 3**). In the thermogravimetric (TG) curve (**Figure 3**), the first stage between 78 and 200°C corresponds to the elimination of 7 water molecules, the second stage from 200 to 322°C is due to the evolving of 2 water molecules and the last stage of dehydration from 322 till 400°C is due to the departure of 1 remaining water molecules.

The derivative of the TG curve, DTG, of $Mn_3(P_3O_9)_2.10H_2O$ under atmospheric pressure and at a heating rate 10°C. min^{-1} (**Figure 3**) contains three peaks due to the dehydration of $Mn_3(P_3O_9)_2.10H_2O$. The first intensive peak in the domain 76 – 200°C, at 172°C is due to the departure of 7 water molecules. The second weak peak in the range 200 – 322°C, at 222°C is due to the evolving of 2 water molecules. The third medium peak in the range 322 – 400°C, at 332°C is due to the evolving of 1 remaining water molecule.

Figure 4, showing the differential thermal analysis (DTA) curve of $Mn_3(P_3O_9)_2.10H_2O$ under atmospheric pressure and at a heating rate 10°C. min^{-1}, reveals three endothermic peaks and one exothermic effect. The first peak is endothermic and well pronounced at 179°C corresponds to the loss of 7 water molecules.

Table 8 Attribution of the observed valence IR frequencies (cm^{-1}) of the P_3O_9 ring (C_1) in $Mn_3(P_3O_9)_2.10H_2O$

M. G.			Δν (cm^{-1})			ν (cm^{-1}) in $Mn_3(P_3O_9)_2.10H_2O$	
D_{3h}			^{16}Oi-^{18}Oi	^{31}P-^{33}P	^{16}Oe-^{18}Oe	C_1	Main
νcal (cm^{-1})	I/Imax	Mode (IR, Ra)			Mode (IR, Ra)		Movement
1287.75	55.3	$A''_2(+,-)$	0.23	18.71	38.80 → A(+,+)	1297	ν_{as} PO_2
1271.80	0.00	E ″(-,+)	0.03	17.97	38.78 → A(+,+)	1274	ν_{as} PO_2
1271.79	0.00		0.03	17.98	38.78 → A(+,+)	1269	ν_{as} PO_2
						1211	
1225.00	100	E ′(+,+)	45.95	9.61	1.02 → A(+,+)		ν_{as} POP
1224.94	100		45.95	9.71	1.02 → A(+,+)		ν_{as} POP
1168.89	0.00	A'_1(-,+)	0.10	12.87	41.33 → A(+,+)	1166	ν_s PO_2
1108.24	5.85	E ′(+,+)	9.82	6.24	45.49 → A(+,+)	1117	ν_s PO_2
1108.21	5.85		9.82	6.24	45.49 → A(+,+)	1103	ν_s PO_2
1059.25	0.00	A'_2(-,-)	48.22	6.28	0.24 → A(+,+)	977	ν_{as} POP
						880	combination
780.69	18.35	E ′(+,+)	12.10	15.32	4.53 → A(+,+)	760	ν_s POP
780.68	18.35		12.11	15.32	4.54 → A(+,+)	743	ν_s POP
670.86	0.00	A'_1(-,+)	11.43	7.76	10.67 → A(+,+)	670	ν_s POP

Δν (cm^{-1}) : effect of the isotopic substitution; Δν (cm^{-1}) : difference between the calculated value of the frequency before and after the substitution; M. G. : molecular group.

The second peak, at 190°C, is exothermic and correspounds to the crystallisation of the cyclotetraphosphate of manganese, $Mn_2P_4O_{12}$, and the manganese diphosphate, $Mn_2P_2O_7$. This crystallization is proved by X-Ray diffraction and Infrared analyses. The third peak is endothermic, medium and large at 230°C is due to the removal of 2 water molecules. The fourth endothermic peak is weak, observed at 340°C is due to the evolving of 1 remaining water molecule. The characteristic temperatures at maximum dehydration rates, in the DTA curve, coincide with those of the derivative of the TG curve, DTG.

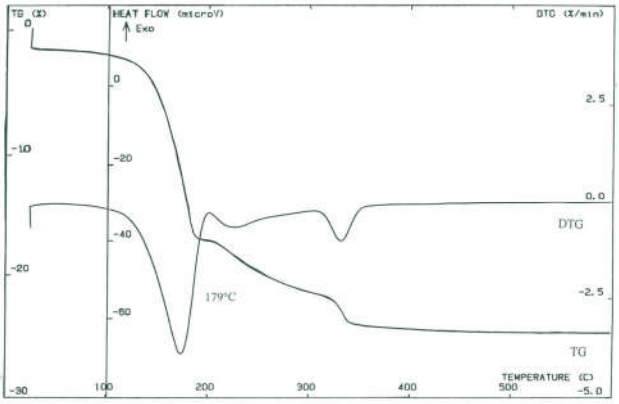

Figure 3 TGA (TG-DTG) curves of $Mn_3(P_3O_9)_2.10H_2O$ at rising temperature (10°C min^{-1})

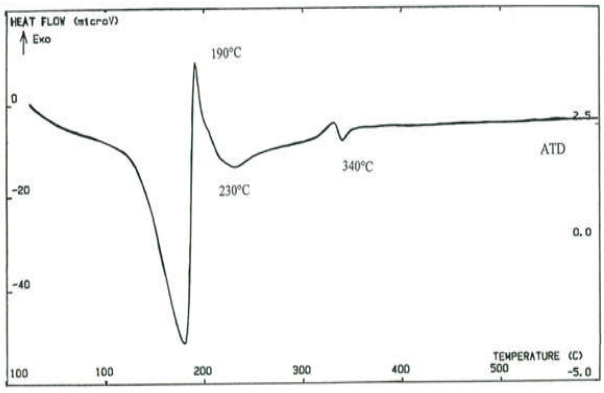

Figure 4 DTA curve of $Mn_3(P_3O_9)_2.10H_2O$ at rising temperature (10°C min^{-1})

Differential scanning calorimetry

The differential scanning calorimetry, DSC, for $Mn_3(P_3O_9)_2.10H_2O$ at rising temperature 5°C. min^{-1} and under atmospheric pressure shows two endothermic peaks and one exothermic effect (**Figure 5**). The first peak is endothermic and observed at 122°C with an enthalpy variation of 14.37 kcal. mol^{-1}, is due to the removal of water molecules. The second peak is exothermic, situated at 188°C with an enthalpy variation of -3.54 $kcal.mol^{-1}$, is due to the crystallisation of the cyclotetraphosphate of manganese, $Mn_2P_4O_{12}$, and the manganese diphosphate, $Mn_2P_2O_7$. This crystallization is observed in the DTA curve at 190°C. The third peak, observed at 307°C, is endothermic with an enthalpy variation of 22.65 $kcal.mol^{-1}$ and corresponds to the dehydration of the title compound $Mn_3(P_3O_9)_2.10H_2O$

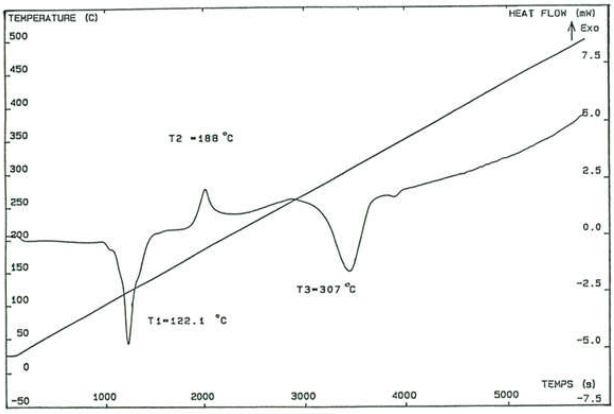

Figure 5 Differential scanning calorimetry DSC curve of $Mn_3(P_3O_9)_2.10H_2O$ at rising temperature (5°C.min^{-1})

Estimation of the thermodynamic function

Various equations of kinetic analyses are known such as Kissinger's method [41], Kissinger-Akahira-Sunose (KAS) [42], Ozawa [43], Coats-Redfern [44] and Van Krevelen *et al.* [45] methods. Especially, the Ozawa and KAS equations were well described and widely used in the literature; therefore, these methods are selected in studying the kinetics of thermal dehydration of the title compound. So, water loss kinetic parameters were evaluated using the Kissinger-Akahira-Sunose (KAS) [42] and Ozawa [43] methods, from the curves $\ln(v/T^2_m) = f(1/T_m)$ and $\ln(v) = f(1/T_m)$ (**Figures. 6 and 7**), where v is the heating rate and T_m the sample temperature at the thermal effect maximum. The characteristic temperatures at maximum dehydration rates, Tm in °C, at different heating rates from the DTA curves of $Mn_3(P_3O_9)_2.10H_2O$ are given in **Table 9.**

From these temperatures and according to the Kissinger-Akahira-Sunose (KAS) [42] and Ozawa [43] methods, the apparent activation energies of dehydration were calculated for the cyclotriphosphate $Mn_3(P_3O_9)_2.10H_2O$. For the Kissinger-Akahira-Sunose (KAS) [42] method, the slope of the resulting straight line of the curve: $\ln(v/T^2_m) = f(1/T_m)$ (**Figure 6**), equals to : $-E_a/R$, allows the apparent activation energy to be calculated (**Table 10**). Concerning the Ozawa [43] method, the slope of the resulting straight line on the curve: $\ln(v) = f(1/T_m)$ (**Figure. 7**), equals to -1.0516E/R, allows also the apparent activation energy to be calculated by this second way (**Table 10**). The equations used for the two methods are the following:

$$Ln\left(\frac{v}{T^2_m}\right) = Ln\left(\frac{AR}{E}\right) - \left(\frac{E}{R}\right)\left(\frac{1}{T_m}\right) \quad \text{for KAS [42]} \quad (1)$$

$$Ln(v) = Ln\left(\frac{AR}{1.0516E}\right) - 1.0516\left(\frac{E}{R}\right)\left(\frac{1}{T_m}\right) \quad \text{forOZAWA [43]} \quad (2)$$

The pre-exponential factor or Arrhenius constant (A) can be calculated from both KAS [42] and Ozawa [43] methods. The related thermodynamic functions can be calculated by using the activated complex theory (transition state) of Eyring [46-48]. The following general equation can be written [48]:

$$A = \left(\frac{e\chi\, k_B T_m}{h}\right) exp\left(\frac{\Delta S^*}{R}\right) \quad (3)$$

where e is the Neper number (e = 2.7183), χ is the transition factor, which is unity for the monomolecular reaction, k_B is the

Boltzmann constant ($k_B = 1.3806 \times 10^{-23}$ J K^{-1}), h is Plank's constant ($h = 6.6261 \times 10^{-34}$ J s), T_m is the peak temperature of the DTA curve, R is the gas constant (R = 8.314 J K^{-1} mol^{-1}) and ΔS^* is the entropy change of transition state complex or entropy of activation. Thus, the entropy of activation may be calculated as follows:

$$\Delta S^* = RLn\frac{Ah}{e\chi\, k_B T_m} \quad (4)$$

The enthalpy change of transition state complex or heat of activation (ΔH^*) and Gibbs free energy of activation (ΔG^*) of decomposition were calculated according to Eqs. (5) and (6), respectively:

$$\Delta H^* = E^* \quad R\,T_m \quad (5)$$

$$\Delta G^* = \Delta H^* \quad T_m \Delta S^* \quad (6)$$

Where, E^* is the activation energy E_a of both KAS [42] and Ozawa [43] methods. The values of the activation energy are gathered in **Table 10**. Thermodynamic functions were calculated from Eqs. (4), (5) and (6) and summarized in **Table 11**. The negative values of ΔS^* from two methods for the dehydration step reveals that the activated state is less disordered compared to the initial state.

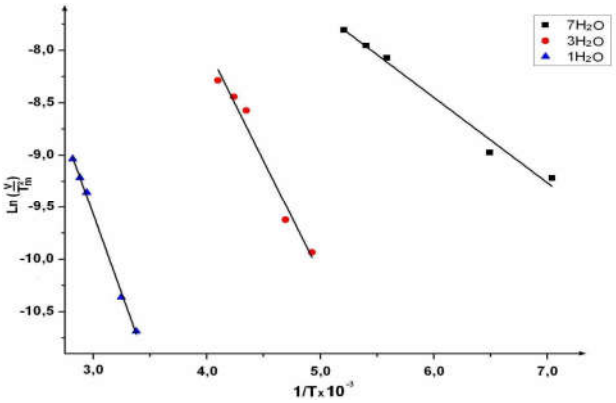

Figure 6 $Ln(v/T_m^2) = f(1/T_m)$ representation of the dehydration thermal effect of the cyclotriphosphate $Mn_3(P_3O_9)_2.10H_2O$

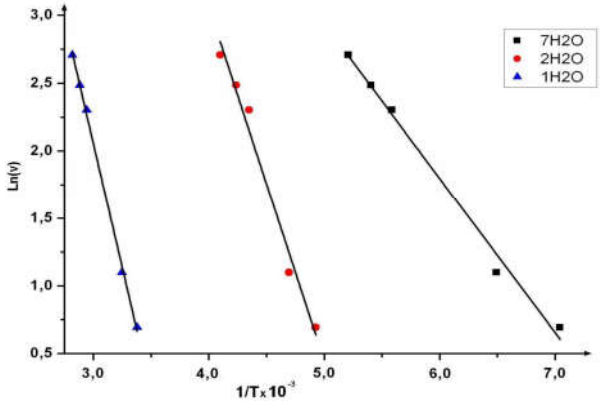

Figure 7 $Ln(v) = f(1/T_m)$ representation of the dehydration thermal effect of the cyclotriphosphate $Mn_3(P_3O_9)_2.10H_2O$

These ΔS^* values suggest a large number of degrees of freedom due to rotation which may be interpreted as a « slow » stage [48-50] in this step. The positive values of ΔG^* at all studied methods are due to the fact that, the dehydration processes are not spontaneous. The positivity of ΔG^* is controlled by a small activation entropy and a large positive activation enthalpy according to the Eq. 6. The endothermic peaks in DTA data agree well with the positive sign of the activation enthalpy (ΔH^*). The estimated thermodynamic functions ΔS^* and ΔG^* (**Table 11**) from two methods are different to some extent due to the different pre-exponential factor of about 10^7. While ΔH^* (**Table 11**) exhibits an independent behavior on the pre-exponential factor as seen from exhibiting nearly the same value.

Table 9 Characteristic temperatures at maximum dehydration rates, T_m in °C, at different heating rates from the DTA curve of $Mn_3(P_3O_9)_2.10H_2O$

$Mn_3(P_3O_9)_2.10H_2O$					
Heating rate *v*	2°C/min	3°C /min	10°C /min	12°C /min	15°C /min
First peak	415	427	452	458	468
Second peak	476	486	503	509	517
Third peak	569	581	613	620	628

Table 10 Activation energy values Ea, pre-exponential factor (A) and correlation coefficient (r^2) calculated by Ozawa and KAS methods for the dehydration of $Mn_3(P_3O_9)_2.10H_2O$

$Mn_3(P_3O_9)_2.10H_2O$						
Model	Ozawa method			KAS method		
	Ea /kJ. mol^{-1}	$A.10^7/min^{-1}$	r^2	Ea/kJ. mol^{-1}	A/min^{-1}	r^2
First peak	9.03	0.65	0.996	6.77	23.00	0.993
Second peak	20.70	197.65	0.991	18.07	4492.87	0.987
Third peak	29.00	171.72	0.999	25.12	1820.66	0.999

Table 11 Values of ΔS^*, ΔH^* and ΔG^* for dehydration step of $Mn_3(P_3O_9)_2.10H_2O$ calculated according to Ozawa and KAS equations

$Mn_3(P_3O_9)_2.10H_2O$						
Model	Ozawa method			KAS method		
	ΔS^* (J. K^{-1}.mol^{-1})	ΔH^* (kJ.mol^{-1})	ΔG^* (kJ.mol^{-1})	ΔS^* (J. K^{-1}.mol^{-1})	ΔH^* (kJ.mol^{-1})	ΔG^* (kJ.mol^{-1})
First peak	-82.63	23.78	75.67	-197.00	19.90	143.62
Second peak	-79.84	16.40	57.68	-187.88	13.78	110.90
Third peak	-82.63	23.78	75.68	-197.00	19.90	143.62

Step manner study

The thermal behavior of $Mn_3(P_3O_9)_2.10H_2O$ was also studied in a step manner of temperature by X-ray diffraction and IR absorption spectrometry between 20 and 1000°C. X-ray diffraction patterns recorded after annealing for 36 hours at different temperatures reveal that $Mn_3(P_3O_9)_2.10H_2O$ is stable up to 80°C **Figure. 1a**). The removal of 7 water molecules of hydration of $Mn_3(P_3O_9)_2.10H_2O$, observed in the temperature range 100-160°C, destroyed the crystalline network and brings to an intermediate amorphous phase [51] which does not diffract the X-ray (**Figure. 1b**), nor exhibits the IR absorption bands characteristic of a cyclic phosphate $P_3O_9^{3-}$ (**Figure. 2b**) [33, 34, 35]. The amorphous product is, according to Van Wazer [51], probably a mixture of manganese oxide MnO and pentoxide phosphorus P_2O_5. After the evolving of the 2 water molecules, between 180-250°C, the atomic rearrangement of MnO and P_2O_5 occurs and provokes the crystallization of a mixture of condensed phosphates $Mn_2P_4O_{12}$ [52] and $Mn_2P_2O_7$ [53]. The latter result is confirmed by X-ray diffraction (**Figure. 1c**) and IR absorption spectrometry (**Figure. 2c**). In fact, the bands appearing in the IR absorption

spectrum of $Mn_3(P_3O_9)_2.10H_2O$, heated between 180-250°C, charecterize easily the structure of a mixture of anions $P_2O_7^{4-}$ and $P_4O_{12}^{4-}$. At 320°C, after the total dehydration and the departure of one remaining water molecule, the X-Ray diffraction and Infrared analyses prove that the final product, of the dehydration of the cyclotriphosphate $Mn_3(P_3O_9)_2.10H_2O$, is the cyclotetraphosphate of manganese $Mn_2P_4O_{12}$. $Mn_2P_4O_{12}$ is stable until its melting point at 980°C.

$Mn_2P_4O_{12}$was prepared, otherwise, using the method of Thilo and Grunze [54]. Stoichiometric quantities of $(NH_4)_2HPO_4$ and $MnCO_3$ are well ground and mixed, and very progressively heated to 350°C to expel ammonia and water vapor. The heating is then resumed up to 400°C, and this temperature is maintained with intervening grindings until a pure phase is obtained, as checked by X-ray diffractometry and IR absorption spectrometry. $Mn_2P_4O_{12}$was obtained as polycristalline samples.

$Mn_2P_4O_{12}$was also obtained by S. Belaaouad [55,56] during the thermal dehydration and calcination of $Mn(NH_4)_4(P_3O_9)_2.6H_2O$ under atmospheric pressure at 500°C.

Interpretation of The Ir Spectrum of Manganese Cyclotetraphosphate $MN_2P_4O_{12}$ Vibrational Analysis of The Cycle $P_4O_{12}^{4-}$ isolated with local Symmetry C_1

The X-ray diffraction structural study [52] showed that the cyclotetraphosphate of manganese, $Mn_2P_4O_{12}$ crystallizes in the monoclinic system, Z = 4, with space group $C_{2/c}$ (C^6_{2h}), with the following lattice parameters: a = 11.883 (1) Å - b = 8.588 (2) Å - c = 10.137 (1) Å, β = 119.21 (2) °.
The crystal lattice contains 4 cycles $P_4O_{12}^{4-}$ with symmetry C_i. All the atoms occupy the sites " 8f " of symmetry C_1 except manganese Mn atoms, which are non equivalent, half occupy the 4 sites "e" of symmetry C_i and the other half occupy the 4 sites "d" of symmetry C_2.

According to E. STEGER and A. SIMON [57], the highest symmetry which the anion $P_4O_{12}^{4-}$ can possess is D_{4h}. For this idealized symmetry the reduced representation is: $\Gamma = 4A_{1g} + 2A_{2g} + 3B_{1g} + 4B_{2g} + 4E_g + A_{1u} + 3A_{2u} + 3B_{1u} + 2B_{2u} + 6E_u$. The separation of normal modes of vibration into stretching and bending modes, $\Gamma = \Gamma_{stretching} + \Gamma_{bending}$, of the cycle $P_4O_{12}^{4-}$ was also given by the authors [58]:

$\Gamma_{stretching} = 2A_{1g} + A_{2g} + B_{1g} + 2B_{2g} + E_g + A_{2u} + B_{1u} + 3E_u$.
$\Gamma_{bending} = 2A_{1g} + A_{2g} + 2B_{1g} + 2B_{2g} + 3E_g + A_{1u} + 2A_{2u} + 2B_{1u} + 2B_{2u} + 3E_u$.

In the case of the "isolated" cycle $P_4O_{12}^{4-}$ with symmetry C_i, The group theory predicts 42 normal modes : Γ int = 21 Au + 21 Ag. The mode Au is active only in IR and the mode Ag is active only in Raman. The separation of normal modes of vibration of the isolated cycle with symmetry C_i is given in

Table 12

It is clear from this analysis that the site symmetry of the $P_4O_{12}^{4-}$ cycle is C_i. The group theory predicts two IR observed frequencies (2Au) and two Raman frequencies (2Ag) in each of the four domains of stretching vibrations. The site group C_i is centrosymmetric, no IR / Raman coincidence is possible (**Table 13**).

Table 12 Separation of the normal modes of vibration, IR and Raman activities of the cycle $P_4O_{12}^{4-}$ isolated with symmetry C_i[57]

	IR	Raman
Internal vibration modes of cycle with symmetry C_i	21 A_u	21 A_g
Stretching modes	8 A_u	8 A_g
Bending modes	13 A_u	13 A_g

The experimental IR spectrum of $Mn_2P_4O_{12}$ prepared by dry method and that obtained during the dehydration of $Mn(NH_4)_4(P_3O_9)_2.6H_2O$ between 320 and 970°C are the same. It shows, three very distinct spectral regions, in the domain of stretching vibrations of the cycle (1400-650 cm^{-1}):

- From 1330 to 1180 cm^{-1}: in this vibrations domain ν_{as} OPO^-, 3 frequencies are observed (1315, 1301 and 1275 cm^{-1}),
- From 1180 to 970 cm^{-1}: in these two vibrations domains $\nu_s OPO^-$ and $\nu_{as}POP$, 4 frequencies are observed (1116, 1101 cm^{-1}) and (1048, 1017 cm^{-1}),
- From 850 to 700 cm^{-1}: vibrations domain of ν_s POP, three frequencies are observed at 733 cm^{-1}, 712 cm^{-1} and 669 cm^{-1}.

The position and the profile of the bands situated at 733 and 712 cm^{-1} for the stretching vibrations ν_s POP suggest that the ring $P_4O_{12}^{4-}$ has the symmetry C_i or C_{2h}. In fact, all the other known symmetries S_4, C_{2v} and C_1, present in the domain of the stretching vibrations ν_s POP, in addition to the two bands at 733 and 712 cm^{-1}, a band around 800 cm^{-1} [58]. But for both the symmetries C_i and C_{2h} of an isolated $P_4O_{12}^{4-}$ ring, two frequencies are predicted in each of the four domains of the stretching vibrations (ν_{as} OPO^-, ν_s OPO^-, ν_{as} POP, ν_s POP) of the ring $P_4O_{12}^{4-}$ (**Table 13**). The IR spectrum of $Mn_2P_4O_{12}$ shows three frequencies in the domain of the stretching vibrations ν_{as} OPO^- : 1330-1180 cm^{-1}. These frequencies are observed at 1315, 1301 and 1275 cm^{-1}. The site symmetry C_i doesn't allow the explanation of the three frequencies observed in the domain of the stretching vibrations ν_{as} OPO^-. Therefore, we make the analysis of the vibrations of the crystalline lattice in order to take into account the interaction between the four cycles of the crystalline lattice of $Mn_2P_4O_{12}$.

Analysis of the vibrations of the manganese cyclotetraphosphate $Mn_2P_4O_{12}$

The crystalline lattice of $Mn_2P_4O_{12}$ contains 4 cycles $P_4O_{12}^{4-}$ with symmetry C_i, Z = 4, while the primitive lattice contains only 2 cycles $P_4O_{12}^{4-}$. The analysis of the vibrations by the method of factor group (C_{2h}) leads to the results gathered in

Table 14

For the two cycles of the primitive lattice, the group theory leads to the existence of 42 IR active modes (21Au + 21Bu) and the same number of modes in Raman (21Ag + 21Bg). No IR / Raman coincidence is possible for the factor group (C_{2h}) centrosymmetric.

During the passage from the isolated cycle with symmetry C_i to the primitive lattice, each band with mode Au active in IR or mode Ag active in Raman should lead respectively to a doublet

(Au + Bu) or (Ag + Bg) according to the correlation scheme as follows:

Correlation diagram: molecular group (D_{4h}) – Site group (C_i) – factor group (C_{2h})

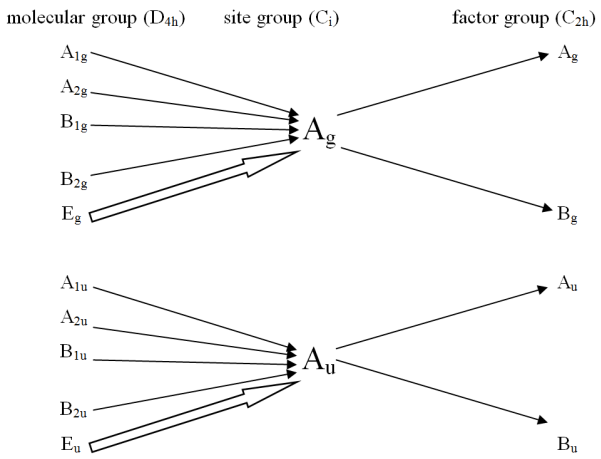

It is useful to have a clear idea about the way the stretching vibration modes are corresponding for the idealized isolated cycle D_{4h} and the isolated cycle in the crystal with site symmetry C_i and then when the coupling is established, optionally, between the cycles in the crystal with space group $C_{2/c}$ (C^6_{2h}) (**Table 13**).

Table 13 Comparison of the stretching vibration modes of the cycle P_4O_{12} «isolated" with local symmetry C_i with the two cycles of the primitive lattice interacting with each other in $Mn_2P_4O_{12}$

Vibrations description	Cycle P_4O_{12} isolated with ideal symmetry D_{4h}	Site symmetry C_i	Group factor C_{2h}
	IR Ra	IR Ra	IR Ra
ν_{as} OPO$^-$	A_{2u} IR - → A_u IR -		Au IR - / Bu IR -
	B_{1u} - - → A_u IR -		Au IR - / Bu IR -
	Eg - Ra → Ag - Ra		Ag - Ra / Bg - Ra
	Eg - Ra → Ag - Ra		Ag - Ra / Bg - Ra
ν_s OPO$^-$	A_{1g} - Ra → A_g - Ra		Ag - Ra / Bg - Ra
	B_{2g} - Ra → A_g - Ra		Ag - Ra / Bg - Ra
	Eu IR - → Au IR -		Au IR - / Bu IR -
	Eu IR - → Au IR -		Au IR - / Bu IR -
ν_{as} POP	A_{2g} - - → A_g - Ra		Ag - Ra / Bg - Ra
	B_{2g} - Ra → A_g - Ra		Ag - Ra / Bg - Ra
	Eu IR - → Au IR -		Au IR - / Bu IR -
	Eu IR - → Au IR -		Au IR - / Bu IR -
ν_s POP	A_{1g} - Ra → A_g - Ra		Ag - Ra / Bg - Ra
	B_{1g} - Ra → A_g - Ra		Ag - Ra / Bg - Ra
	Eu IR - → Au IR -		Au IR - / Bu IR -
	Eu IR - → Au IR -		Au IR - / Bu IR -

The results of this theoretical analysis is that the possible interaction or vibrational couplings between the two cycles $P_4O_{12}^{4-}$ of the primitive lattice $Mn_2P_4O_{12}$ should occur on the IR spectrum and the Raman spectrum by the existence of four observed frequencies in each of the 4 domains of the stretching vibrations (ν_{as} OPO$^-$, ν_s OPO$^-$, ν_{as} POP, ν_s POP) of the $P_4O_{12}^{4-}$ ring.

Table 14 Separation of the normal modes of vibration, IR and Raman activities of the $P_4O_{12}^{4-}$ cycles in $Mn_2P_4O_{12}$

	IR	**Raman**
Active internal modes (total)	$27A_u + 27B_u$	$25A_g + 26B_g$
Lattice vibration modes	$6A_u + 6B_u$	$A_g + 2B_g$
Libration modes of the cycles	---	$3A_g + 3B_g$
Internal vibration modes of the cycles	$21A_u + 21B_u$	$21A_g + 21B_g$
Stretching modes	$8A_u + 8B_u$	$8A_g + 8B_g$
Bending modes	$13A_u + 13B_u$	$13A_g + 13B_g$

The experimental IR spectrum of $Mn_2P_4O_{12}$ shows two frequencies in each of the two fields of the stretching vibrations ν_s OPO$^-$ (1116, 1101 cm^{-1}), ν_{as} POP (1048, 1017 cm^{-1}) and three frequencies in each of the two domains of the stretching vibrations ν_{as} OPO$^-$ (1315, 1301 and 1275 cm^{-1}) and ν_s POP (733, 712 and 669 cm^{-1}). The assignment of the stretching frequencies of the $P_4O_{12}^{4-}$ cycles on the basis of factor group C_{2h} is given in **Table 15**. Vibrational couplings are therefore effective only for antisymmetric vibrations, ν_{as} OPO$^-$, involving external oxygen atoms of the ring which are the most susceptible to interact with a neighbor ring through bonds between cation and external oxygen atoms of the $P_4O_{12}^{4-}$ cycle. But, for the vibrations of the groups P-Oi-P, ν_{as} POP and ν_s POP, couplings are less important and can be observed as two bands instead of four theoretically expected. The results of the analysis of the IR spectrum related to the symmetry of the ring $P_4O_{12}^{4-}$ in the manganese cyclotetraphosphate, $Mn_2P_4O_{12}$, are in good agreement with the structural resolution [52].

Table 15 Assignments of the stretching vibrations of the $P_4O_{12}^{4-}$ cycles in $Mn_2P_4O_{12}$

Vibrations description	Cycle P_4O_{12} isolated with ideal symmtry D_{4h}	Site symmetry C_i	Group factor C_{2h}	Observed IR frequencies	Calculated frequencies S_4 [59]
	IR Ra	IR Ra	IR Ra	IR	IR Ra
ν_{as} OPO$^-$	A_{2u} IR - → A_u IR -		Au IR - / Bu IR -	1315 / 1301	1275 -
	B_{1u} - - → A_u IR -		Au IR - / Bu IR -	1275	1261 -
	Eg - Ra → Ag - Ra		Ag - Ra / Bg - Ra		
	Eg - Ra → Ag - Ra		Ag - Ra / Bg - Ra		
ν_s OPO$^-$	A_{1g} - Ra → A_g - Ra		Ag - Ra / Bg - Ra		- 1128
	B_{2g} - Ra → A_g - Ra		Ag - Ra / Bg - Ra		- -
	Eu IR - → Au IR -		Au IR - / Bu IR -	1116 / 1101	1121 -
	Eu IR - → Au IR -		Au IR - / Bu IR -		
ν_{as} POP	A_{2g} - - → A_g - Ra		Ag - Ra / Bg - Ra		
	B_{2g} - Ra → A_g - Ra		Ag - Ra / Bg - Ra		
	Eu IR - → Au IR -		Au IR - / Bu IR -	1048 / 1017	994 -
	Eu IR - → Au IR -		Au IR - / Bu IR -		
ν_s POP	Eu IR - → Au IR -		Au IR - / Bu IR -	733 / 712 / 669	739 -
	Eu IR - → Au IR -		Au IR - / Bu IR -		
	A_{1g} - Ra → A_g - Ra		Ag - Ra / Bg - Ra		
	B_{1g} - Ra → A_g - Ra		Ag - Ra / Bg - Ra		

Comparison of the thermal behavior of cyclotriphosphates hydrated type $M_3^{II}(P_3O_9)_2.10H_2O$ (M^{II} = Ca and Cd), $Ba_3(P_3O_9)_2.6H_2O$, $Pb_3(P_3O_9)_2.3H_2O$, $Cd_3(P_3O_9)_2.14H_2O$ and $Sr_3(P_3O_9)_2.7H_2O$ with $Mn_3(P_3O_9)_2.10H_2O$.

In our laboratory, to date, the thermal behavior was studied for six cyclotriphosphates hydrated type $M^{II}_3(P_3O_9)_2.10H_2O$ (M^{II} = Ca and Cd) [6, 8], $Ba_3(P_3O_9)_2.6H_2O$ [5], $Pb_3(P_3O_9)_2.3H_2O$ [7] and $Cd_3(P_3O_9)_2.14H_2O$ [7] and $Sr_3(P_3O_9)_2.7H_2O$ [55, 56]. It would be useful to compare the thermal behavior of these six cyclotriphosphates with that of $Mn_3(P_3O_9)_2.10H_2O$. For the cyclotriphosphates $M_3^{II}(P_3O_9)_2.10H_2O$ (M^{II} = Ca and Cd) [6,8], $Ba_3(P_3O_9)_2.6H_2O$ [5], $Pb_3(P_3O_9)_2.3H_2O$ [7], $Cd_3(P_3O_9)_2.14H_2O$ [7] and $Sr_3(P_3O_9)_2.7H_2O$ [55, 56], after the removal of a partial quantity of water molecules by thermal dehydration, they all lead to amorphous products in X-ray diffraction and don't exhibit the IR absorption bands characteristic of cyclic phosphates $P_3O_9^{3-}$. The final products of the total thermal dehydration, for $Ca_3(P_3O_9)_2.10H_2O$ [6,8], $Ba_3(P_3O_9)_2.6H_2O$ [5], $Pb_3(P_3O_9)_2.3H_2O$ [7] and $Cd_3(P_3O_9)_2.14H_2O$ [7] and $Sr_3(P_3O_9)_2.7H_2O$ [55, 56], are the corresponding long-chain polyphosphates $[M^{II}(PO_3)_2]_\infty$ (M^{II} = Ca, Ba, Pb, Cd and Sr) with an exception in the case of $Mn_3(P_3O_9)_2.10H_2O$ and $Cd_3(P_3O_9)_2.10H_2O$ [8] which lead to their corresponding anhydrous cyclotetraphosphates respectively $Mn_2P_4O_{12}$ and $Cd_2P_4O_{12}$.

It's the first time where a cyclotriphosphate P_3O_9 is converted to a cyclotetraphosphate P_4O_{12} by thermal dehydration.

CONCLUSION

$Mn_3(P_3O_9)_2.10H_2O$ has been prepared by the method of ion exchange-resin. Thermal behavior of $Mn_3(P_3O_9)_2.10H_2O$ has been studied by X-ray diffraction, infrared spectroscopy, thermal analyses TGA-DTA and differential scanning calorimetry. After a partial dehydration, $Mn_3(P_3O_9)_2.10H_2O$ leads to an amorphous phase by X-ray diffraction and IR spectroscopy. With further increase in temperature, the latest amorphous phase is converted to a mixture of $Mn_2P_2O_7$ and $Mn_2P_4O_{12}$. Finally the mixture $Mn_2P_2O_7$ and $Mn_2P_4O_{12}$ leads by heating at higher temperature to $Mn_2P_4O_{12}$. So, the final product of the total thermal dehydration of $Mn_3(P_3O_9)_2.10H_2O$ under atmospheric pressure is its corresponding anhydrous cyclotetraphosphate $Mn_2P_4O_{12}$. The thermodynamic and kinetic features (apparent activation energy, entropy activation, heat activation and Gibbs free energy of activation) of the thermal dehydration of $Mn_3(P_3O_9)_2.10H_2O$ have been determined by Ozawa and KAS methods. The vibrational spectra of $Mn_3(P_3O_9)_2.10H_2O$ and $Mn_2P_4O_{12}$ were examined and interpreted in the domain of the stretching vibrations of the P_3O_9 and P_4O_{12} rings. A comparison of the thermal behavior of cyclotriphosphates hydrated type $M_3^{II}(P_3O_9)_2.10H_2O$ (M^{II} = Ca and Cd), $Ba_3(P_3O_9)_2.6H_2O$, $Pb_3(P_3O_9)_2.3H_2O$, $Cd_3(P_3O_9)_2.14H_2O$ and $Sr_3(P_3O_9)_2.7H_2O$ with $Mn_3(P_3O_9)_2.10H_2O$ was performed. $Pb_3(P_3O_9)_2.3H_2O$, $Cd_3(P_3O_9)_2.14H_2O$, $Ca_3(P_3O_9)_2.10H_2O$ and $Ba_3(P_3O_9)_2.6H_2O$ have the same thermal behavior. They all lead to their corresponding long-chain polyphosphates $[M^{II}(PO_3)_2]_\infty$ (M^{II} = Pb, Cd, Ca and Ba). On the contrary, $Mn_3(P_3O_9)_2.10H_2O$ and $Cd_3(P_3O_9)_2.10H_2O$ lead to their corresponding cyclotetraphosphates $M^{II}_2P_4O_{12}$ (M^{II} = Mn, Cd). The results obtained in this paper can be added to previous works on thermal transformations of condensed hydrated cyclophosphates. It's worth noticing that it's the first time where a cyclotriphosphate P_3O_9 ($Mn_3(P_3O_9)_2.10H_2O$) is converted to a cyclotetraphosphate P_4O_{12} ($Mn_2P_4O_{12}$) by thermal dehydration.

References

1. N. EL Horr et A. Durif, C. R. Acad. Sci. Paris., 296(2), 1185 (1983).
2. R. Masse, J. C. Guitel et A. Durif, Acta Cryst., B32, 1892 (1976).
3. M. T. Averbuch-Pouchot and A. Durif, Z. Krist., 174, 219 (1986).
4. I. Tordjman, A. Durif et J. C. Guitel, Acta Cryst., B32, 205 (1976).
5. S. Belaaouad, Y. Lahrir, S. Sarhane and M. Tridane, Phosphorus Research Bulletin Vol. 23, 67-75 (2009).
6. S. Belaaouad, M. Tridane, H. Chennak, R. Tamani, A. Kenz, M. Moutaabbid, Phosphorus Research Bulletin. 21, 60-70 (2007).
7. Aziz Kheireddine, Malika Tridane and Said Belaaouad, Mediterr. J. Chem., 2(4), 549-569 (2013)
8. K. Brouzi, A. Ennaciri, M. Harchrras, K. Sbai, Ann. Chim. Sci. Mat., 28, 159-166, (2003).
9. M. T. Averbuch-Pouchot and A. Durif, Topics in Phosphate Chemistry. World Scientific. Singapore. New Jersey. London. Hong Kong. (1996).
10. A. Durif, Crystal Chemistry of Condensed Phosphates. Plenum Press. New York. (1995).
11. R. Dumon, Le Phosphore et les Composés Phosphorés. Masson. Paris. New York. Barcelone. Milan. (1980).
12. M. Greenblatt, P. P. Tsai, T. Kodama and S. Tanase, Solid State Ionics., 40/41, 444 (1990).
13. A. Jouini, J. C. Gacon, M. Ferid, M. Trabelsi-Ayadi. Opt. Mater. 24, 175, (2003).
14. T. Kitsugi, T. Yamamuro, T. Nakamura, M. Oka. Biomaterials 16, 1101, (1995).
15. B. Jian-Jiang, K. Dong-Wan, H. Kug Sun, J. Europ. Ceram. Soc., 23, 2589, (2003).
16. J. R. Martinelli, F. F. Sene, L. gomes. J. Non-Cryst. Solids., 263, 299, (2000).
17. P. Carmen, P. Gosefina, S. P. regino, R. V. Caridad, S. Natalia.Chem. Mater., 15, 3347, (2003)
18. I. C. Marcu, J. M. Millet, I. Sandulescu. Prog. Catal., 71, 10, (2001).
19. H. Onoda, K. Kojima, H. Nariai. J. Alloys. Comp. , 568, 408-412, (2006)
20. H. Onoda, H. Nariai, H. Maki, I. Motooka. Mater. Chem. and Phys., 73(1), 19, (2002)
21. H. Onoda, A. Takenaka, K. Kojima,H. Nariai. Mater. Chem. and Phys., 82(1), 194, (2003)
22. M. Tridane. Doctorat National. Faculté des Sciences Ben M'sik. Casablanca. Maroc. (2006).
23. N. Stock. Z. Naturforsch. 57b, 187, (2002).
24. M. Trojan, D. Brandova, M. Kuchler. Proceedings of the State Conference on Industrial
25. M. Trojan, D. Brandova. Thermochim. Acta 161, 11, (1990).
26. M. Trojan. Thermochim. Acta 159, 13, (1990).

27. M. Trojan, D. Brandova, Z.Solc. Thermochim. Acta 110, 343, (1987).
28. R. K. Malkani, K. S. Suresh, G.V.Bakore. J. Inorg. Nucl. Chem., 39, 621, (1977)
29. M. Tridane and S. Belaaouad, J. Mater. Environ. Sci. 6 (12), 3476-3482 (2015)
30. B. Boonchom, C. Danvirutai, S. Maensiri. Mater. Chem. and Phys., 109, 404-410, (2008)
31. M. Tridane, A. Kheireddine, I. Fahim, H. Moutaabbid, M. Moutaabbid, EL. M. Tace, A. Charaf, M. Radid, F. Salhamen, S. Benmokhtar. Verres, Céramiques
32. A. Jouini and A. Durif, C. R. Acad. Sci. Paris., 297 II, 573 (1983).
33. K. Sbai, Thèse d'Etat. Faculté des Sciences Mirande. Dijon. France. (1984).
34. W. Bues et H. W. Gehrke, Z. Anorg. Allgem. Chem., 288, 307 (1956).
35. P. Tarte, A. Rulmont, K. Sbai and M. H. Simonot-Grange, Spectrochimica Acta., 43A(3), 337 (1987).
36. K. Sbai, A. Abouimrane, A. Lahmidi, K. EL Kababi, M. Hliwa and S. Vilminot, Ann. Chim. Sci. Mat., 25. Supplt. 1, S139 (2000).
37. M. T. Averbuch - Pouchot, A. Durif and J.C. Guitel, Acta. Cryt., B32, 1894 (1976).
38. M. Tridane, Thèse de troisième cycle. Faculté des Sciences Ben M'Sik. Casablanca. Maroc. (1999).
39. M. J. S. Dewar and W. Thiel, J. Am. Chem. Soc., 99, 4899 (1977).
40. K. Sbai and S. Belaaouad, J. Phys. Chem. Sol., (64), 981 (2003).
41. H. E. Kissinger, Anal. Chem., **29,** 1702 (1957).
42. T. Akihira, T. Sunose, Trans. 1969 ; Res Report Chiba Inst. Technol. (Sci. Technol.), **16,** 22 (1971).
43. T. A. Ozawa, Bull. Chem. Soc. Jpn., **38,** 1881 (1965).
44. A. W. Coats, J. P. Redfern, Nature G, **20,** 68 (1964).
45. D. W. Van Krevelns, P.J.Hoftijzer, Trans. I. Chem. E., **32,** 5360 (1954).
46. D. Young, Decomposition of Solids, Academia Prague, (1984).
47. J. Rooney, J. Eyring, J. Mol. Catal. A. Chemical., **L1,** 96 (1995).
48. B. Boonchom, J. Chem. Eng. Data., **53,**1533 **(**2008).
49. L. Valaev, N. Nedelchev, K. Gyurova, M. Zagorcheva, J.Anal. Appl. Pyrol., **81,** 253 (2008).
50. P. Noisong, C. Danavirutai, T. Boonchom, Solid State Sci., **10,** 1598 (2008).
51. J. R. Van Wazer and K. A. Holst, J. Amer. Chem. Soc., 72, 639 (1950).
52. TH. HINSCH, W. GUSE and H. SAALFELD. J. Cryst. Growth, 79, 205, (1986).
53. T. STEFANIDIS and A. G. NORD. Acta. Cryst. C49, 1995-1999, (1984).
54. E. Thilo und I. Grunze, Z. Anorg. Allgem. Chem., 290(5-6), 209 (1957).
55. S. Belaaouad, Thèse de troisième cycle. Faculté des Sciences Ben M'Sik. Casablanca. Maroc. (1993).
56. *S. Belaaouad, Thèse d'Etat. Faculté des Sciences Ben M'Sik. Casablanca. Maroc. (2002).*
57. E. Steger Et A. Simon.Z. Anorg. Allg. Chem., 291, 76, (1957).
58. G. Foumakoye, R. Cahay Et P. Tarte. Spectrochim. Acta., 46a(8), 1245-1257, (1990).
59. Kh. Kh. Mulglaglaiev, A. N. Lazarev Et A. P. Mirgodsku. Izv. Acad. Nauk. Sssr Neorg. Mater., 10(4), 563, (1974).

****

How to cite this article:

Bouchra Gourja *et al.*2016, Study of the Structural Modifications of Cyclophosphates of Manganese From $Mn_3 (P_3O_9)_2.10H_2O$ TO $MN_2P_4O_{12}$ During Thermal Behavior Process By Infrared Spectroscopy. *Int J Recent Sci Res.* 7(9), pp. 13462-13473.